Biomechanical Evaluation of Subcrestal Placement of Dental Implants: In Vitro and Numerical Analyses

Chun-Ming Chu,* Jui-Ting Hsu,* Lih-Jyh Fuh,* and Heng-Li Huang*

Background: This study investigates the effect of depth of insertion in subcrestal cortical bone (SB) and thickness of connected cortical bone (CB) for a subcrestal implant placement on bone stress and strain using statistical analyses combined with experimental strain-gauge tests and numerical finite element (FE) simulations.

Methods: Three experimental, artificial jawbone models and 72 FE models were prepared for evaluation of bone strain and stress around various equicrestal and subcrestal implants. For in vitro tests, rosette strain gauges were used with a data acquisition system to measure bone strain on the bucco-lingual side. The maximum von Mises stresses in the bone were statistically analyzed by analysis of variance for FE models.

Results: The experimental bone strains reduced significantly (22% to 49%) as the thickness of CB increased. FE analyses indicated that the suggested CB thickness for efficiently minimizing bone stress was 0.5 to 2.5 mm. The results for the depth of SB were not absolute because obvious stress reductions only presented at a certain range of depth (0.6 to 1.2 mm).

Conclusion: Within the limitations of this study, increasing the thickness of CB and maintaining the depth of SB within a limited range can provide the benefit of decreasing the stress and strain in surrounding bone for subcrestally placed implants. *J Periodontol 2011;82:302-310.*

KEY WORDS

Biomechanics; dental implants; dental stress analysis; finite element analysis; implants, experimental; in vitro.

* School of Dentistry, China Medical University and Hospital, Taichung, Taiwan.

Dental implants have been applied in dentistry for over 30 years, since the introduction of osseointegration by Brånemark et al.[1] For two-piece implant systems, the implant placement provides the advantage of primary wound closure of soft tissue over the implant, which allows the connection at the interface between implant and bone (osseointegration) to be achieved without disturbing bone growth. After osseointegration, abutment and prosthetic components are then placed in the implant to perform the occlusal function. However, in this kind of implant surgery, typically 1 to 1.5 mm of peri-implant bone loss occurs during healing and after the first year of implant placement.[2,3] Studies have indicated that many possible factors affect peri-implant bone loss, including reformation of the biologic width,[4,5] the presence of a microgap between implant and abutment in two-stage implants,[6,7] implant overloading,[8-10] and peri-implantitis.[11,12]

Certain implant designs have been proposed for preserving the level of the marginal bone around implants, such as platform switching[13] and subcrestal placement.[14-17] A conical abutment (or Morse-taper connection) has been introduced as one type of platform-switching design, which means that connecting a reduced-diameter abutment to an implant can result in a circumferential horizontal mismatch around the implant shoulder. It has been proposed to reduce the loss of

doi: 10.1902/jop.2010.100040

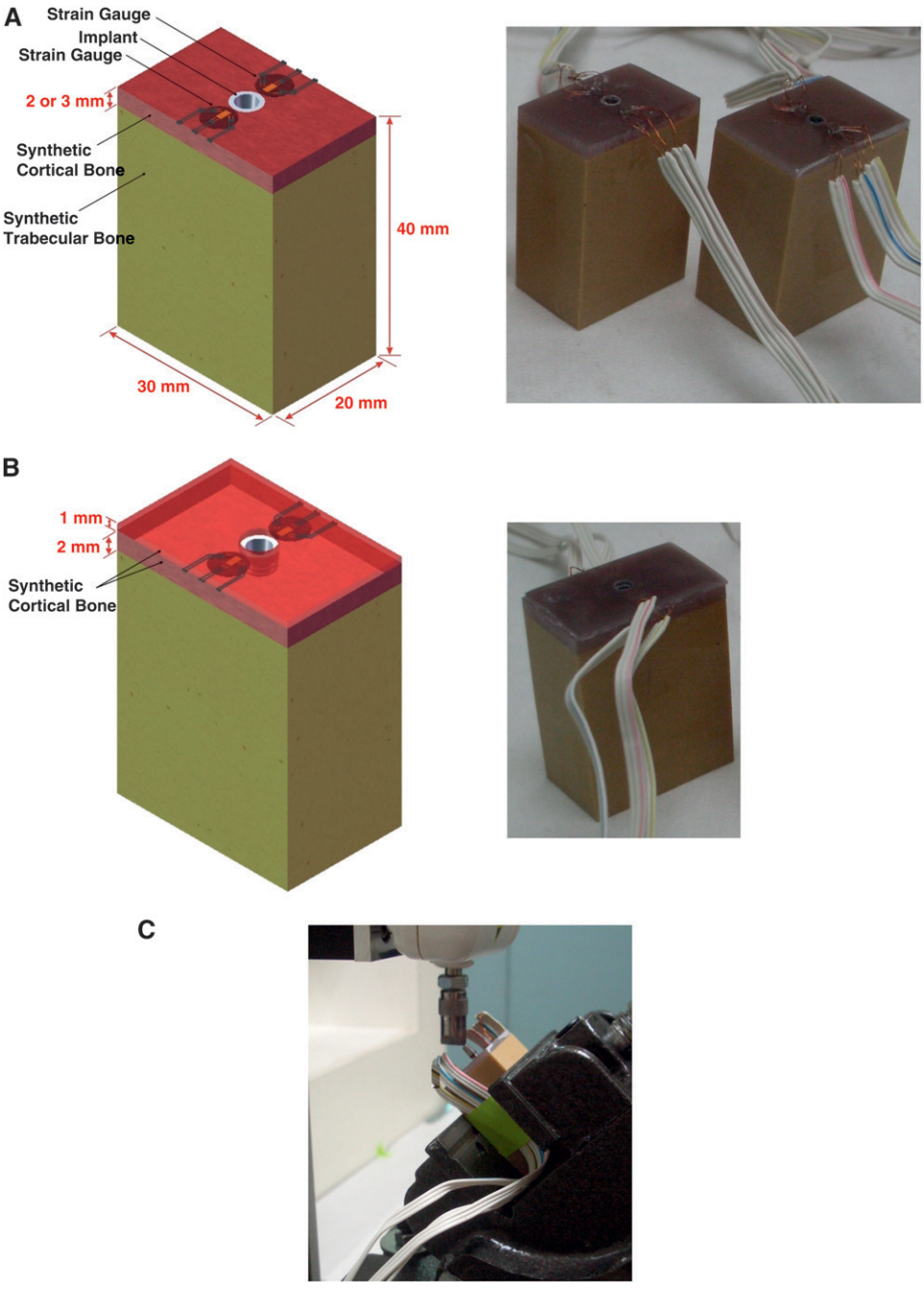

Figure 1.
A) *Schematic of the equicrestal models. Model 1 (right) and Model 2 (left) with 2- and 3-mm thickness of cortical bone, respectively.* ***B)*** *Schematic of the subcrestal models. Compared to the equicrestal models, another 1-mm-thick cortical shell was fixed on the top surface as Model 3 with a total 3-mm thickness of cortical bone.* ***C)*** *Application of 45-degree lingual lateral force to the top of the implant.*

crestal bone height because the inflammatory cell infiltrate moves inwardly at the implant–abutment gap and away from crestal bone to prevent bone loss.[13] In addition, an implant with a conical abutment recently has been considered with the treatment of subcrestal placement and in some animal studies has been found to have a positive impact on crestal bone preservation.[14-17]

The use of subcrestal placement of two-stage implants has been found to have a small amount of additional bone loss[14] and can even have a positive impact on crestal bone preservation.[15] Pontes et al.[16,17] indicated that deeper implant insertion does not jeopardize the peri-implant ridge height and soft tissue. Welander et al.[18,19] demonstrated that osseointegration might occur at or above the level of the implant–abutment junction when implant components with suitable surface characteristics are subcrestally placed. In addition, Barros et al.[20] showed that the subcrestal placement of a contiguous Morse-taper connection with platform switching was more capable of preserving the interimplant crestal bone. Because the subcrestal implant placement changes the traditional design of the connection (equicrestal placement) between implant and bone, the stress and strain distribution from the implant to the bone might be influenced when occlusal loading occurs. However, the biomechanical effect of subcrestal implant placement with conical abutment on bone stress and strain is still a controversial issue and remains to be investigated.

The aim of this study is to elucidate the effects of subcrestal implant placement for various insertion depths and different cortical bone thickness on stress and strain performances of surrounding bone using in vitro experiments and three-dimensional finite element (FE) analyses.

MATERIALS AND METHODS

In Vitro Experiments

Three experimental bone models were prepared. In Model 1 (2-mm-thick cortex) and Model 2 (3-mm-thick

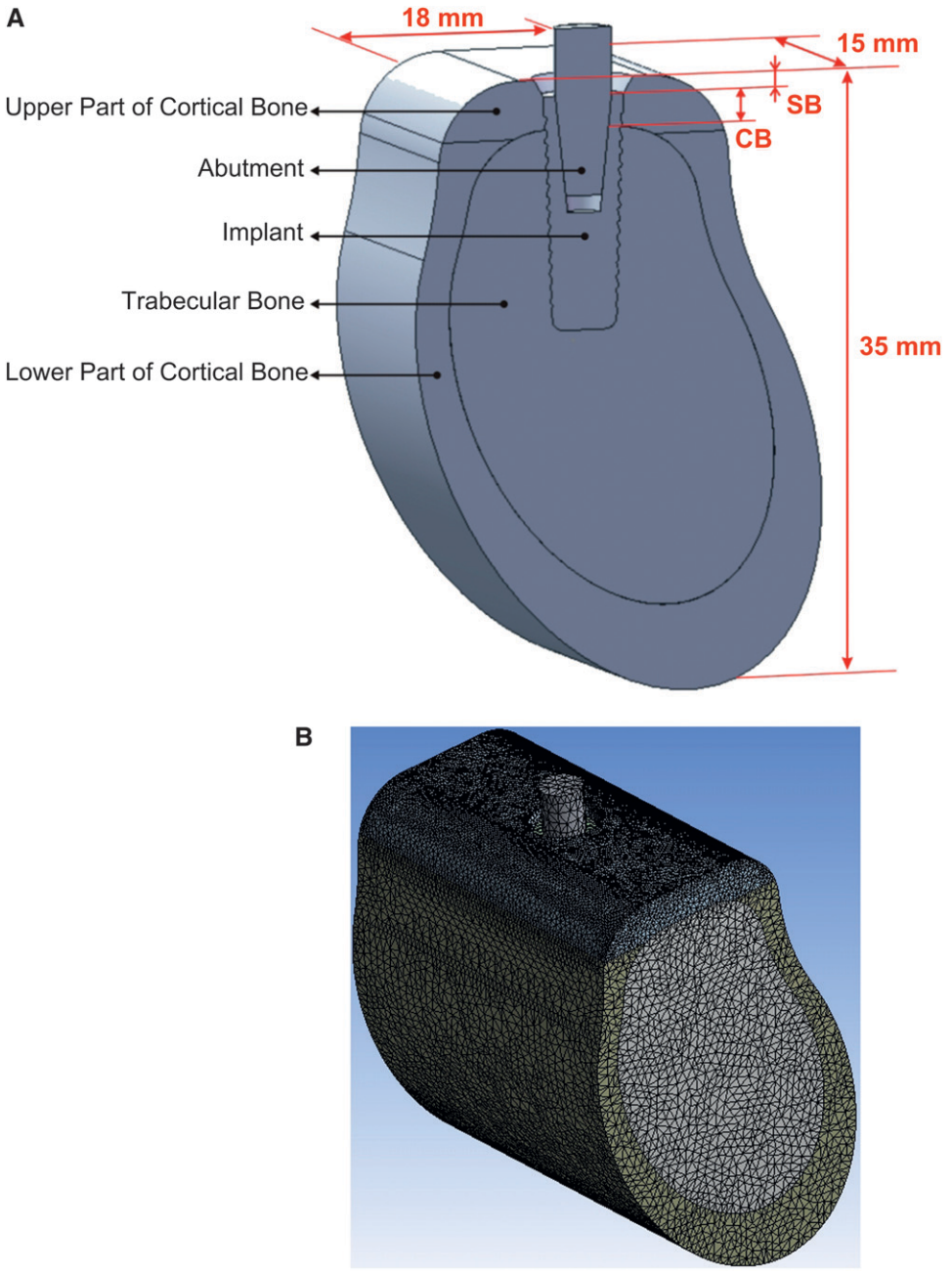

Figure 2.
A) *Cross-sectional view of the solid model, showing its detailed dimensions.* ***B)*** *FE mesh model.*

cortex), the implants were placed at the level of the crest cortical bone (equicrestal implant placements) (Fig. 1A). Therefore, 2- and 3-mm-thick commercially available synthetic cortical shells† were prepared for attachment to the trabecular bone specimen‡ to simulate jaw bone. After drilling appropriate holes, 3.5 × 11 mm of the commercially available implants§ were inserted and Morse-taper abutments‖ were used for connection to the implant. To measure the strain of bone around the implant, rectangular rosette strain gauges¶ (1 mm in length and 1.5 mm in width) were attached to the buccal and lingual sides of the crestal region of cortical shell around the implant by using cyanoacrylate cement# (Fig. 1).

For subcrestal placement, 2 mm of cortical thickness of bone model were prepared as Model 1, and then an additional 1-mm-thick cortical shell was attached on the top of the bone model to create a 1-mm subcrestal bone thickness for Model 3 (Fig. 1B). For all models, cyanoacrylate cement** was used to bind the surfaces of implant and bone model to simulate a bonded (osseointegration) interface. The dimensions of the bone block were 20 × 30 × 40 mm in the bucco-lingual, mesio-distal, and apical-coronal directions, respectively.

A customized jig was designed with an adjustable screwing device so that a 45-degree lingual oblique force could be applied in the experiments. Each loading procedure involved applying a force of 170 N[21] to the conical abutment using a universal testing machine†† with a head speed of 1 mm per minute (Fig. 1C). Strain-gauge signal process[22] related to the three independent strains ε_a, ε_b, and ε_c measured by the three gauges comprising the rosette strain gauge was sent to the data acquisition system‡‡ and analyzed by the associated software.§§ Each measurement was repeated three times. The maximum (ε_{max}) and minimum (ε_{min}) principal strains were obtained as follows:

† Model 3401, Pacific Research Laboratory, Vashon Island, WA.
‡ Model 1522-05, Pacific Research Laboratory.
§ ANKYLOS Plus Implant A11 implant system, DENTSPLY Friadent, Mannheim, Germany.
‖ ANKYLOS 3102-1050, DENTSPLY Friadent.
¶ KFG-1-120-D17-11L3M3S, Kyowa, Tokyo, Japan.
# CC-33A, Kyowa.
** CC-33A, Kyowa.
†† JSV-H1000, Japan Instrumentation System, Nara, Japan.
‡‡ CompackDAQ, National Instruments, Austin, TX.
§§ LabVIEW SignalExpress, National Instruments.

$$\varepsilon_{max} = 1/2(\varepsilon_a + \varepsilon_c) + 1/2\sqrt{[(\varepsilon_a - \varepsilon_c)2 + (2\varepsilon_b - \varepsilon_a - \varepsilon_c)^2]} \quad (1)$$

$$\varepsilon_{min} = 1/2(\varepsilon_a + \varepsilon_c) - 1/2\sqrt{[(\varepsilon_a - \varepsilon_c)2 + (2\varepsilon_b - \varepsilon_a - \varepsilon_c)^2]} \quad (2)$$

Statistical Analyses

One-way analysis of variance (ANOVA) and Duncan multiple comparisons were used to assess differences in the peak values of principal strains between the models. All analyses were performed using a statistical package of commercial software‖‖ with an α value of 0.05.

FE Analysis

Computer-aided design (CAD) software¶¶ was used to construct a model of the bone block based on a cross-section image of the human mandible in the molar region (Fig. 2A).[23] The trabecular core was surrounded by the cortical shell. The cortical shell was divided into two parts: subcrestal cortical bone (SB) and connected cortical bone (CB). The SB was on top of the part of the crestal bone that did not touch the implant surface, and the CB was the remaining part of the cortex that was connected to the implant surface. Nine depths of SB were simulated, from 0 (equicrestal) to 1.6 mm, and eight thicknesses of CB were simulated, from 0.5 to 4 mm (Table 1 and Fig. 2A). Therefore, a total of 72 FE models were created for the analyses.

A screw-type of root-form implant (5 × 14 mm) was constructed using CAD software. After obtaining all of the models by applying Boolean operations to the variables, the corresponding solid models were exported in the IGES format to the commercial FE software## to generate the FE models using 10-node tetrahedral h-elements.*** The interfacial condition between the implant and CB was set as bonded to simulate ideal osseointegration. The contact condition between the abutment and implant was set with a frictional coefficient (μ) of 0.3.[24] The implant and abutment were modeled as titanium with homogeneous and isotropic elastic properties. The cortical bone and trabecular bone were considered to be anisotropic (i.e., with properties varying in different directions) (Table 2).[25,26] The mesial and distal surfaces of the bone models were constrained as the boundary conditions. The loading condition was applied on the top surface of the abutment. A 170-N oblique force was applied at 45 degrees to the long axis of the implant. Based on the convergence testing process[27] for appropriate results, the element size was 0.2 mm for the upper part of cortical bone and 0.5 mm elsewhere in the model (Fig. 2B).

ANOVA was performed to determine how the depths of SB and the thickness of CB influenced the maximum von Mises stresses in bone. Probability values of <0.05 were considered to be significant. The correlation coefficients (R^2) and regressions were used to determine the relationship between bone stress and various types of SB and CB.

Table 1.

SB and CB Variables in FE Models

SB (mm)	0	0.2	0.4	0.6	0.8	1	1.2	1.4	1.6
CB (mm)	0.5	1	1.5	2	2.5	3	3.5	4	—

SB indicates the depth of cortical bone that did not touch the implant surface. CB is the distance of the remaining part of the cortex that was connected to the implant surface.

Table 2.

Material Properties in the FE Analyses

Material	Young Modulus E (MPa)		Poisson Ratio ν		Shear Modulus G (MPa)	
Cortical bone	E_x	19,400	ν_{xy}	0.390	G_{xy}	5,700
			ν_{yz}	0.300		
	E_y	12,600	ν_{xz}	0.390	G_{yz}	4,850
			ν_{yx}	0.253		
	E_z	12,600	ν_{zy}	0.300	G_{xz}	5,700
			ν_{zx}	0.253		
Trabecular bone	E_x	1,148	ν_{xy}	0.055	G_{xy}	68
			ν_{yz}	0.010		
	E_y	210	ν_{xz}	0.322	G_{yz}	68
			ν_{yx}	0.010		
	E_z	1,148	ν_{zy}	0.055	G_{xz}	434
			ν_{zx}	0.322		
Titanium	110,000		0.30			

The subscripts indicate the *x*, *y*, and *z* axes represent the mesial-distal, superior-inferior, and buccal-lingual directions, respectively.

RESULTS

In Vitro Experiments

The mean ± SD values of the maximum (ε_{max}) and minimum (ε_{min}) principal strains on the buccal and lingual sides are shown in Figure 3. The peak values of bone strains are the minimum principal strains of bone at the buccal side around an implant (Buccal_ε_{min}), and those peak strains were all significant in ANOVA (P<0.001) and Duncan multiple comparisons among three models (Fig. 3). The peak value of bone strain was 48% lower in Model 2 (with a thicker cortical bone) than in Model 1 (–2012 ± 114), and 38% lower in Model 3 (with 1-mm-thick subcrestal bone) than in Model 1.

‖‖ Version 9.1, SAS Institute, Cary, NC.
¶¶ SolidWorks 2008, SolidWorks Corporation, Concord, MA.
ANSYS Workbench 10.0, Swanson Analysis, Huston, PA.
*** ANSYS solid 187, Swanson Analysis.

FE Analyses

Both thickness of CB and depth of SB significantly (P <0.0001) affected the bone stress. The maximum von Mises stresses of bone in the 72 FE models are listed in Table 3. The mean values of bone stresses in the models containing various depths of SB but with the same thickness of CB (bottom row in Table 3) indicate that the stresses reduced as the thickness of CB increased, but the rate of the stress reduction gradually declined. The regression equation between the stress and the thickness of CB was approximately quadratic, with a strong correlation (R = 0.84) (Fig. 4A).

The mean stresses of bone in the models containing various thickness of CB but with the same depths of SB (right column in Table 3) indicate that the bone stress reduced as the depth of SB increased. However, no correlation between them was apparent when the depth of SB was <0.6 mm. The regression equation between the stress and the depth of SB was approximately linear, but with a weak correlation (R = 0.37) (Fig. 4B).

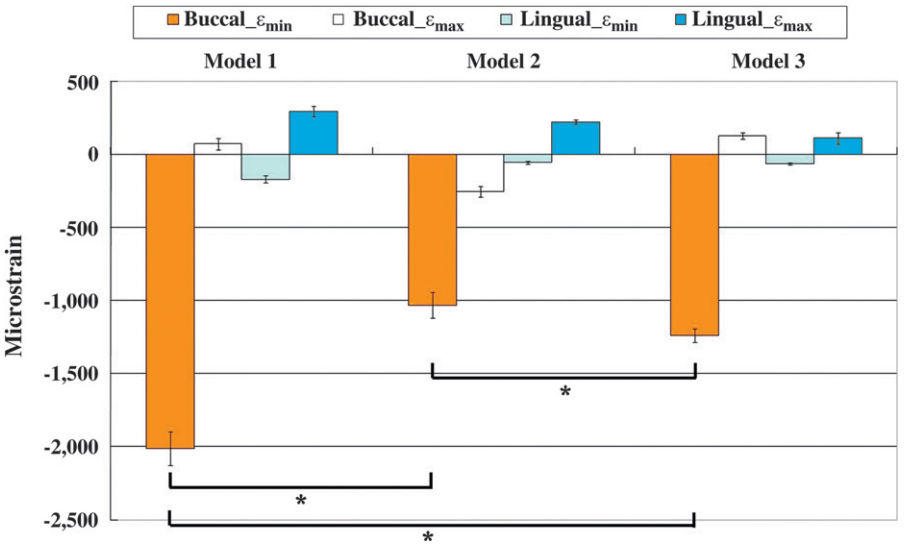

Figure 3.
Mean values (error bars indicate SDs) of the maximum (tensile) and minimum (compressive) principal strains on the buccal and lingual sides of the four experimental models. ANOVA analysis shows the significant difference (P <0.001) in the peak strains (the minimum principal strains) of bone. Asterisks demonstrate significant differences in Duncan multiple range test among the three models.

DISCUSSION

There are few surgical techniques that have been developed to

Table 3.

Maximum von Mises Stresses (MPa) of Bone in the Models and SD in SB and CB Models With the Same Variable Values

Measurement	CB0.5	CB1.0	CB1.5	CB2.0	CB2.5	CB3.0	CB3.5	CB4.0	CB Mean	SD
SB0	112.4	68.7	56	45.6	40.6	38.4	36.6	35.9	54.3	26
SB0.2	97.4	80.4	56.7	46.3	42.1	41	38.1	38.4	55.1	22.2
SB0.4	97.2	72.3	52.7	46.4	43.2	40.8	41.5	40	54.2	20.4
SB0.6	70.2	64.1	46.1	41.3	36.4	35.5	32.1	31.6	44.7	14.7
SB0.8	73.6	53.7	37.8	34.5	31.1	30.2	28.3	28.4	39.7	16.1
SB1.0	66.5	55.2	49.6	44.1	39.3	36.1	34.7	33.6	44.9	11.6
SB1.2	58.3	46.3	43.8	36.3	32.2	30.6	31.4	32.3	38.9	9.8
SB1.4	60.1	45.8	37.2	35.9	34	31.8	30.6	29.4	38.1	10.3
SB1.6	57.9	48.3	35.1	33.3	35.1	33.6	32.3	29.2	38.1	9.8
SB Mean	77.1	59.4	46.1	40.4	37.1	35.3	34	33.2		
SD	20.1	12.5	8.2	5.4	4.4	4.1	4.1	4.2		

The numbers after CB and SB represent the amount of CB and SB (e.g., "CB2" means that the model has 2 mm of CB attached to the implant surface). As the increase of CB the bone stress is reduced, and the rate of the stress reduction is gradually declined. In addition, the bone stresses decrease as the SB increases over a certain depth (0.6 mm).

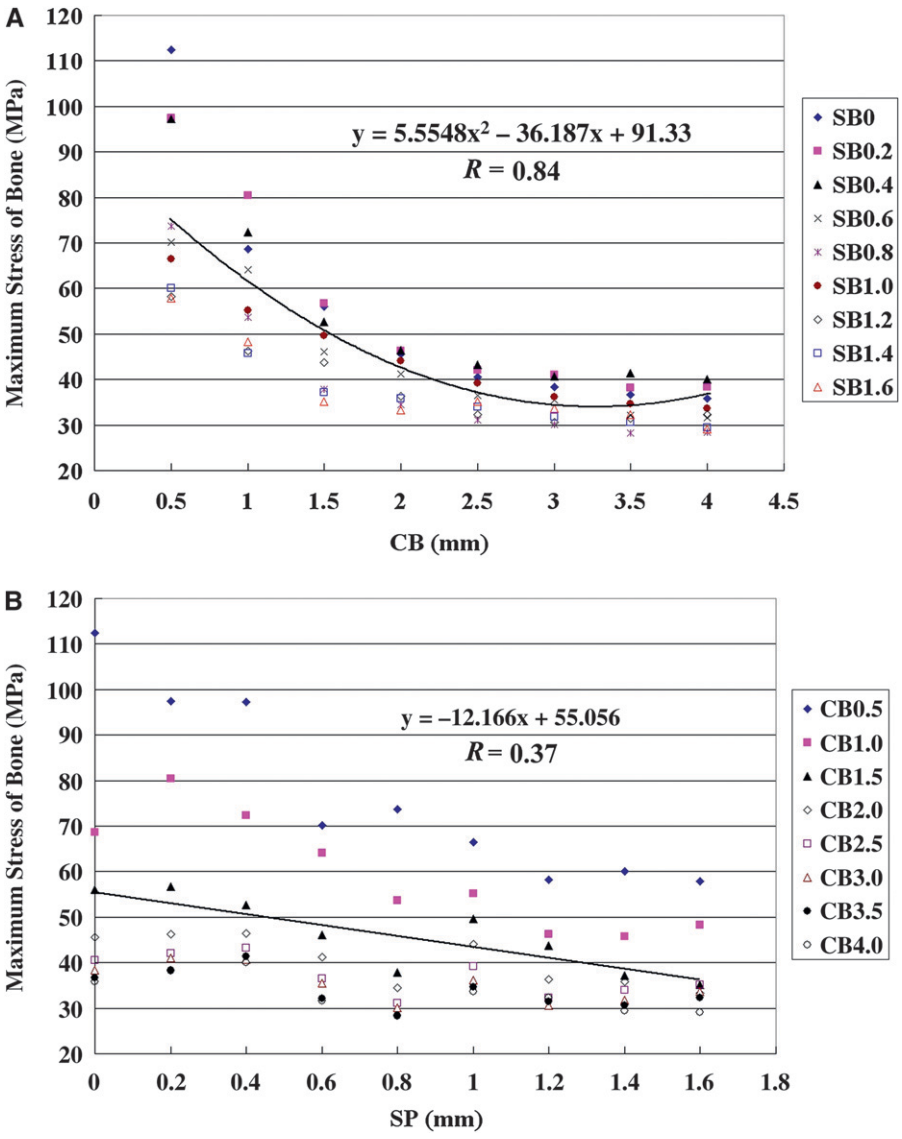

Figure 4.
Scatterplot of maximum von Mises bone stress versus models with various thickness of CB ***(A)*** *and depths of SB* ***(B)****. Black line indicates the quadratic regression equation for all data points.*

preserve peri-implant bone.[28] For example, bone resorption is thought to be lower for a subcrestal placement of implant than for a traditional (equicrestal) placement of implant,[20] but few researchers[29] have investigated subcrestal placement of implant or the underlying biomechanical mechanisms. The present study might be the first to have investigated the biomechanical performances of various subcrestal placements of implants by using experimental strain-gauge measurements and nonlinear FE simulations[30,31] with statistical analyses. In the experimental tests, the strains were measured locally by sensors (i.e., strain gauges) attached at selected locations. The strain gauges were placed on bone near the implant, and hence they were unable to measure the peak value of the bone strain when this occurred within the bone. However, in the FE simulation, the peak values of the strain within bone were easily determined. Nevertheless, an FE approach produces an approximate solution rather than an exact one, and hence the combined techniques of experimental measurements and FE simulations as used in the present study might facilitate the understanding of biomechanical mechanisms related to subcrestal implant placement.

The thickness of CB affects bone stresses and strains in both equicrestal and subcrestal implants. In the experimental tests, bone strain was lower in the model with 3-mm-thick CB (Model 2) than in the model with 2-mm-thick CB (Model 1). In the FE analyses, the thickness of CB also played a major role in stress reduction, especially as it increased from 0.5 to 2.5 mm. These findings are consistent with previous studies indicating that thicker cortical bone reduces stress concentrations around implants.[32,33] However, increasing the CB thickness above 2.5 mm in the models (to 3 and 4 mm) had less effect on stress reduction; compared with 0.5-mm-thick CB (77.1 MPa), the mean stress decreased by 52% for 2.5-mm-thick CB (37.1 MPa), but only by 5% more for 4-mm-thick CB (decrease of 57%; 33.2 MPa). These findings indicate that the bone stress and strain do not reduce linearly as CB increases, with a limited range of CB thickness (<2.5 mm) being sufficient to provide a superior outcome in terms of decreasing the bone stress and strain around the implant.

The subcrestal placement of the implant into the cortical bone (SB) resulted in a length of bone that was not in contact with the implant. The experimental tests of the effects of the SB length showed that the bone strain was lower in the subcrestal implant (Model 3) than in the equicrestal implant (Model 1). Likewise, in the FE simulation the bone stresses decreased as the SB increased over a certain depth (0.6 mm). However, why the bone stress did not reduce with increasing depth for SB >0.6 mm remains unclear

and hence requires further investigation. Nevertheless, this study indicates that results of increasing the depth of SB to decrease the bone stress for a subcrestal implant are not absolute, with only SB depths larger than a certain value seeming to decrease the bone stress. Therefore, with an evaluation of cortical bone thickness by radiograph or cone-beam computed tomography when the total cortical thickness is ≤2.5 mm, CB thickness should be primarily considered, and equicrestal implant placement is recommended rather than subcrestal implant placement from a biomechanics viewpoint. However, for cortical thickness >2.5 mm, a moderate subcrestal implant placement (e.g., 0.6 mm) might be a suggestion for implants to further reduce the bone stress.

Another advantage of a subcrestal implant generally observed in this study is that the peak stress, which might result in bone loss, is distant from the crestal region. Placing an implant subcrestally and using a Morse-taper abutment for the connection (platform switching) can transfer the high-stress area to the subcrestal region and make it narrower, thereby avoiding the stress concentration at the crestal bone around the implant as is usually found in equicrestal implants (Fig. 5). Our findings might help to explain the clinical finding of Weng et al.[15] that the use of a subcrestally placed implant with a Morse-taper connection seemed to avoid a large "dish-shaped" bone defect (resorption). This might be beneficial to reduce the risk of bone loss caused by overloading around implants. However, some factors (e.g., inflammation within the surrounding tissues, reformation of the biologic width, presence of a microgap between implant and abutment, and peri-implantitis) also affect peri-implant bone loss and were not investigated in this study. This requires further investigation.

One limitation of this study is the simplified geometry of the bone model in the experimental tests. Even though the strength of a bone block is similar to that of jaw bone, the strain patterns might vary with the bone geometry. In addition, although the material properties of the FE mandibular model were assumed to be anisotropic, the consideration of the inhomogeneous properties is still needed in future studies. Another limitation was the use of a static occlusal force in the experiments and FE simulations. Although oblique loading has been suggested to represent a realistic occlusal load,[34] chewing movement, especially with dynamic loading simulations, needs to be considered in future investigations.

CONCLUSIONS

Within the limitations of this study, the following conclusions can be drawn. First, increasing the thickness of CB reduces bone stress and strain in both equicrestal and subcrestal placement of implants. However, bone stress and strain do not decrease linearly with increasing CB thickness; only at a certain range of CB thickness (<2.5 mm) can significant reduction occur in the bone stress and strain around the implant. Second, for the results of the subcrestal implant, only at certain depths of SB (0.6 to 1.2 mm)

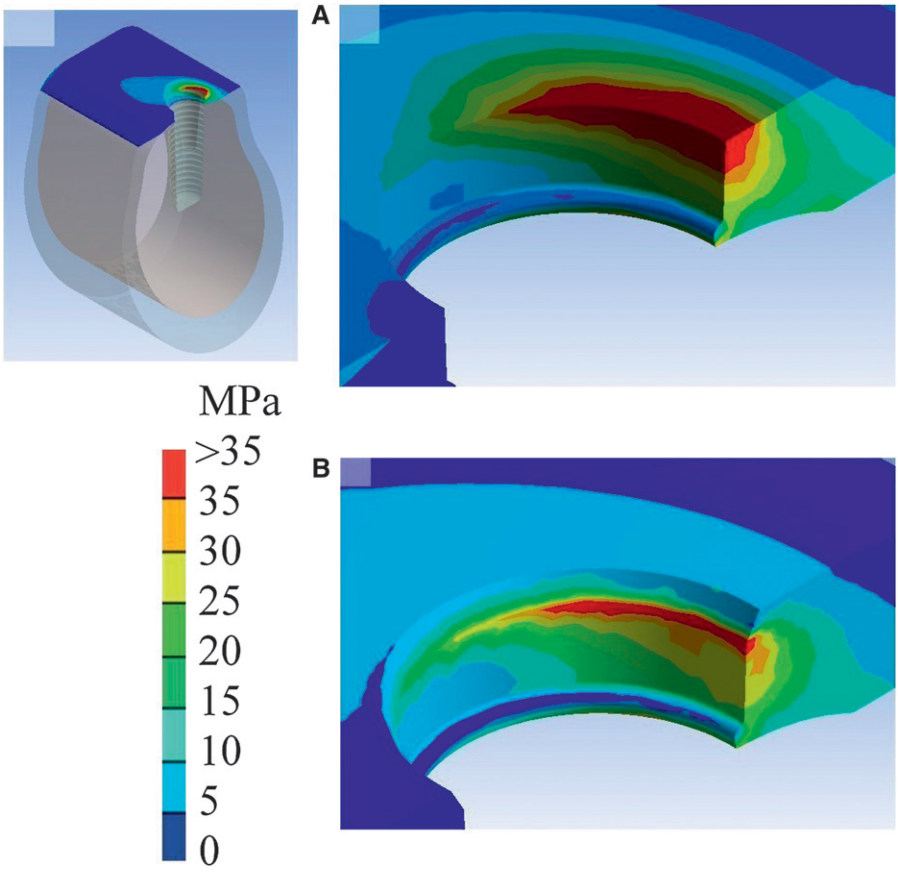

Figure 5.
von Mises stress distributions in the cortical bone in the equicrestal implant model CB1.5/SB0 ***(A)*** *and the subcrestal implant model CB1.5/SB0.4* ***(B)****. A 45-degree of oblique force (170 N) was applied on the top of the implant and dark blue to red colors represent stress values from lower to higher. The result shows that subcrestal implant placement has a smaller area of high (red) bone stresses than equicrestal implant placement.*

is there a benefit to decreasing the surrounding bone stress and strain.

ACKNOWLEDGMENTS

This research was supported by the National Science Council (NSC 98-2320-B-039-005-MY3), a government-funded organization in Taiwan. The authors thank Ms. Kuan-Ting Chen, China Medical University Biostatistics Center, for her help in statistical analyses. The authors report no conflicts of interest related to this study.

REFERENCES

1. Brånemark PI, Adell R, Breine U, Hansson BO, Lindström J, Ohlsson A. Intra-osseous anchorage of dental prostheses. I. Experimental studies. *Scand J Plast Reconstr Surg* 1969;3:81-100.
2. Adell R, Lekholm U, Rockler B, Brånemark PI. A 15-year study of osseointegrated implants in the treatment of the edentulous jaw. *Int J Oral Surg* 1981;10:387-416.
3. Jemt T, Lekholm U, Gröndahl K. 3-year followup study of early single implant restorations ad modum Brånemark. *Int J Periodontics Restorative Dent* 1990; 10(5):340-349.
4. Berglundh T, Lindhe J. Dimension of the periimplant mucosa. Biological width revisited. *J Clin Periodontol* 1996;23:971-973.
5. Tarnow DP, Cho SC, Wallace SS. The effect of inter-implant distance on the height of inter-implant bone crest. *J Periodontol* 2000;71:546-549.
6. Ericsson I, Persson LG, Berglundh T, Marinello CP, Lindhe J, Klinge B. Different types of inflammatory reactions in peri-implant soft tissues. *J Clin Periodontol* 1995;22:255-261.
7. Hermann JS, Schoolfield JD, Schenk RK, Buser D, Cochran DL. Influence of the size of the microgap on crestal bone changes around titanium implants. A histometric evaluation of unloaded non-submerged implants in the canine mandible. *J Periodontol* 2001; 72:1372-1383.
8. Miyata T, Kobayashi Y, Araki H, Ohto T, Shin K. The influence of controlled occlusal overload on peri-implant tissue. Part 4: A histologic study in monkeys. *Int J Oral Maxillofac Implants* 2002;17:384-390.
9. Isidor F. Influence of forces on peri-implant bone. *Clin Oral Implants Res* 2006;17(Suppl. 2):8-18.
10. Heckmann SM, Linke JJ, Graef F, Foitzik CH, Wichmann MG, Weber HP. Stress and inflammation as a detrimental combination for peri-implant bone loss. *J Dent Res* 2006;85:711-716.
11. Nociti FH Jr., Cesco De Toledo R, Machado MA, Stefani CM, Line SR, Gonçalves RB. Clinical and microbiological evaluation of ligature-induced peri-implantitis and periodontitis in dogs. *Clin Oral Implants Res* 2001;12:295-300.
12. Zitzmann NU, Berglundh T, Ericsson I, Lindhe J. Spontaneous progression of experimentally induced periimplantitis. *J Clin Periodontol* 2004;31:845-849.
13. Lazzara RJ, Porter SS. Platform switching: A new concept in implant dentistry for controlling postrestorative crestal bone levels. *Int J Periodontics Restorative Dent* 2006;26(1):9-17.
14. Todescan FF, Pustiglioni FE, Imbronito AV, Albrektsson T, Gioso M. Influence of the microgap in the peri-implant hard and soft tissues: A histomorphometric study in dogs. *Int J Oral Maxillofac Implants* 2002;17: 467-472.
15. Weng D, Nagata MJ, Bell M, Bosco AF, de Melo LG, Richter EJ. Influence of microgap location and configuration on the periimplant bone morphology in submerged implants. An experimental study in dogs. *Clin Oral Implants Res* 2008;19: 1141-1147.
16. Pontes AE, Ribeiro FS, Iezzi G, Piattelli A, Cirelli JA, Marcantonio E Jr. Biologic width changes around loaded implants inserted in different levels in relation to crestal bone: Histometric evaluation in canine mandible. *Clin Oral Implants Res* 2008;19:483-490.
17. Pontes AE, Ribeiro FS, da Silva VC, et al. Clinical and radiographic changes around dental implants inserted in different levels in relation to the crestal bone, under different restoration protocols, in the dog model. *J Periodontol* 2008;79:486-494.
18. Welander M, Abrahamsson I, Berglundh T. Subcrestal placement of two-part implants. *Clin Oral Implants Res* 2009;20:226-231.
19. Welander M, Abrahamsson I, Berglundh T. Placement of two-part implants in sites with different buccal and lingual bone heights. *J Periodontol* 2009; 80:324-329.
20. Barros RR, Novaes AB Jr., Muglia VA, Iezzi G, Piattelli A. Influence of interimplant distances and placement depth on peri-implant bone remodeling of adjacent and immediately loaded Morse cone connection implants: A histomorphometric study in dogs. *Clin Oral Implants Res* 2010;21:371-378.
21. Kawaguchi T, Kawata T, Kuriyagawa T, Sasaki K. In vivo 3-dimensional measurement of the force exerted on a tooth during clenching. *J Biomech* 2007; 40:244-251.
22. Hoffmann K. *An Introduction to Measurements Using Strain Gages*. Darmstadt, Germany: Hottinger Baladwin Messtechnik; 1989:1-257.
23. Eraslan O, Inan O. The effect of thread design on stress distribution in a solid screw implant: A 3D finite element analysis. *Clin Oral Investig* 2010.14:411-416.
24. Alkan I, Sertgöz A, Ekici B. Influence of occlusal forces on stress distribution in preloaded dental implant screws. *J Prosthet Dent* 2004;91:319-325.
25. O'Mahony AM, Williams JL, Spencer P. Anisotropic elasticity of cortical and cancellous bone in the posterior mandible increases peri-implant stress and strain under oblique loading. *Clin Oral Implants Res* 2001;12: 648-657.
26. Huang HL, Chang CH, Hsu JT, Fallgatter AM, Ko CC. Comparison of implant body designs and threaded designs of dental implants: A 3-dimensional finite element analysis. *Int J Oral Maxillofac Implants* 2007; 22:551-562.
27. Huang HL, Hsu JT, Fuh LJ, Tu MG, Ko CC, Shen YW. Bone stress and interfacial sliding analysis of implant designs on an immediately loaded maxillary implant: A non-linear finite element study. *J Dent* 2008;36: 409-417.
28. Hermann F, Lerner H, Palti A. Factors influencing the preservation of the periimplant marginal bone. *Implant Dent* 2007;16:165-175.
29. Baggi L, Cappelloni I, Di Girolamo M, Maceri F, Vairo G. The influence of implant diameter and length on stress distribution of osseointegrated implants related to crestal

bone geometry: A three-dimensional finite element analysis. *J Prosthet Dent* 2008;100:422-431.
30. Hsu JT, Fuh LJ, Lin DJ, Shen YW, Huang HL. Bone strain and interfacial sliding analyses of platform switching and implant diameter on an immediately loaded implant: Experimental and three-dimensional finite element analyses. *J Periodontol* 2009;80:1125-1132.
31. Eser A, Akça K, Eckert S, Cehreli MC. Nonlinear finite element analysis versus ex vivo strain gauge measurements on immediately loaded implants. *Int J Oral Maxillofac Implants* 2009;24:439-446.
32. Holmes DC, Loftus JT. Influence of bone quality on stress distribution for endosseous implants. *J Oral Implantol* 1997;23:104-111.
33. Kitagawa T, Tanimoto Y, Nemoto K, Aida M. Influence of cortical bone quality on stress distribution in bone around dental implant. *Dent Mater J* 2005;24:219-224.
34. Geng JP, Tan KB, Liu GR. Application of finite element analysis in implant dentistry: A review of the literature. *J Prosthet Dent* 2001;85:585-598.

Correspondence: Professor Heng-Li Huang, School of Dentistry, China Medical University and Hospital, 91 Hsueh-Shih Road, 404 Taichung, Taiwan. Fax: 1-886-4-22014043; e-mail: hlhuang@mail.cmu.edu.tw.

Submitted January 25, 2010; accepted for publication August 5, 2010.